Tanzania Journal of Engineering and Technology 2023, **42(1)**:135-145
OPEN ACCESS articles distributed under Creative Commons Attribution Licence [CC BY-ND]
Websites: https://www.ajol.info/index.php/tjet; https://tjet.udsm.ac.tz

ISSN 1821-536X (**print**); ISSN 2619-8789 (**electronic**)
DOI: 10.52339/tjet.v42i1.894

Special Issue – Seventh International Conference on Mechanical and Industrial Engineering (MIE) 2022 Conference, 20 – 21, October 2022, UDSM New Library, Dar es Salaam, TANZANIA

Preparation and Characterization of Microporous Cellulose Membranes as Potential Pathogen Filters

Joshua C. William, Tausi H. Alexander, Lutamyo Nambela, Liberato V. Haule, Bwire S. Ndazi*, and Peresi M. Bulemo*
Department of Mechanical and Industrial Engineering, College of Engineering and Technology, University of Dar es Salaam.
*Corresponding email: pmajura@udsm.ac.tz; bndazi@udsm.ac.tz

ABSTRACT

Growth and development in the textile and fashion industry have resulted in the generation of large amounts of industrial pre-consumer textile wastes. It is estimated that 10 to 20% of textile fabrics are wasted during garment manufacturing, with most of the wastes being burned or landfilled. Reusing pre-consumer fabric wastes is therefore considered a viable approach to alleviate environmental impacts associated with their disposal. To achieve a higher porosity membrane, pre-consumer cotton fabrics were partially dissolved in a solution of dimethyl acetamide (DMAc) and lithium chloride (LiCl), and the resulting fibre suspension was utilized to prepare a microporous cellulose membrane (MCM) through a vacuum filtration method. The suspension comprised a mixture of partially and completely dissolved fibres, which provided the required morphological and structural integrity to the fibrous membranes. The membranes' chemical structure, fibre size, and morphology were characterized based on Fourier transform infrared spectroscopy (FT-IR), light microscope, and field emission scanning electron microscopy (FE-SEM), respectively. The filtration efficiency of the microporous cellulose membranes was evaluated against 500 ppm sodium chloride (NaCl) solutions. The results showed that the filtration efficiency of the membranes ranged between 31.82 and 59.85% for cellulose membranes with 60.2% porosity, suggesting that the membranes could be applied as filters against pathogens upon further improvement.

ARTICLE INFO

Submitted: **June 27, 2022**

Revised: **Sept. 30, 2022**

Presented: **Oct. 20-21, 2022**

Accepted: **Dec. 18, 2022**

Published: **Feb. 25, 2023**

Keywords: *Cellulose, Fibrous membrane, Vacuum filtration, Cellulose dissolution.*

INTRODUCTION

Industrialisation, growing population, and urbanisation combined lead to increased air pollution, especially from particulate matter, which has significantly impacted people's health and quality of life (Kaur and Pandey 2021, Li et al. 2016; Power et al. 2018). In addition, recurrent outbreaks of respiratory diseases also threatened human lives (Adil et al. 2021; Noor and Maniha 2020). Consequently, technological and medical measures are being undertaken to prevent the transmission of respiratory pathogens and air particulate matters' pollution (Piscitelli et al. 2022). Unfortunately, technical measures for dust reduction, suppression, separation, and exhaustion are only effective against fine

dust and do not offer adequate protection against respiratory pathogens (Adil et al. 2021). Filter membranes are therefore simple, and the most effective protective means for people against infection by viruses and airborne particles (Bolashikov and Melikov 2009; Ijaz et al. 2016). On the other hand, the mass production, use and disposal of filter membranes pose adverse environmental problems due to the increasing need for protection against respiratory pathogens (Cornelio et al. 2022, Pandit et al. 2021; Tesfaldet and Ndeh 2022). For example, on February 24, 2020, Wuhan (China), a city of over 11 million people, generated 200 tons of clinical waste in one day, consisting of many discarded filter materials (Saadat et al. 2020). Synthetic filter membranes typically take about 450 years to degrade, damaging the ecosystems as they degrade. (Fan et al. 2018; Wang et al. 2021).

Various techniques for the fabrication of filter membranes have been reported, including melt-blown polypropylene (PP) and non-woven fabrics (Selvaranjan et al. 2021; Song et al. 2022). However, it is difficult to control the fibre distribution and shape with these traditional preparation processes (Giovambattista et al. 2009). The pore size of filters made from these methods is relatively not small enough to filter fine particles, such as respiratory pathogens or aerosols, because of large fibres sizes and the wide distribution of their diameters (Borojeni et al. 2022; Wang et al. 2021). Although the filtration performance of the membranes can be improved by adding electret finishing (Sanyal and Sinha-Ray 2021; Zhou et al. 2022), the charge induced by the electret treatment gradually dissipates during use and cleaning, significantly affecting the stability of the filter performance and the reusability of the fibrous membrane (Wang et al. 2018; Xiao et al. 2014).

Conversely, fibrous membranes prepared via vacuum filtration can achieve high filtration performance owing to their interconnected pores (Bonfim et al. 2021; Gopakumar 2017). Many studies have been reported on the fabrication of membranes by combining vacuum filtration and hot-pressing to achieve fibre membranes with high filtration efficiency (Mautner et al. 2015). For example, bio-based fibre membranes made from polyamide fibres have the highest filtration efficiency of up to 99.995% (Liu et al. 2015; Wang et al. 2021). This implies that biodegradable and environmentally benign fibrous membranes, such as cellulose materials, can exhibit high filtration efficiency for pathogens. Therefore, this study aims to develop an environmentally friendly membrane from waste cotton fabric for the filtration of pathogens as well as to eradicate environmental pollution associated with the incineration of waste cotton fabrics.

MATERIALS AND METHODS

Materials

The following materials and chemicals were used to prepare the microporous membranes. Pre-consumer waste cotton fabrics were collected from the 21st Century Textile Mills garment section in Morogoro, Tanzania. Lithium chloride (LiCl, ≥ 98.3%), hydrogen peroxide (H_2O_2, ≥ 97%), and ethanol (EtOH, ≥ 99%) were obtained from LOBA Chemie Pvt. Ltd, whereas *N*, *N*-dimethylacetamide (DMAc, ≥98%), sodium lauryl sulfate ($C_{14}H_{29}NaO5S$, ≥ 99%), and Millipore filter membranes (Nylon, VWR 413, 0.45 µm pore size, Lutterworth, UK) were obtained from LOBA chemical supplier. Distilled water was obtained from the Department of Chemical and Process Engineering, University of Dar es Salaam.

Equipment and Apparatus

The following equipment and apparatus were used in this study: Domestic blender (ES-2255), accurate analytical balance (Wintech, JA203P), Oven (Zuk-OV23A, China), and Mathis Labomat BFA-12

infrared beaker dyeing machine. Other equipment includes a magnetic stirrer with a hot plate (MS-7 H-550, Biobase, China), light microscope (RBM-117M-Biobase, China), FT-IR spectrophotometers Alpha II (Bruker Optics, Germany), digital thickness gauge (MGJDC018, Yiyang, China), and vacuum filtration pump (Edwards RV5, United Kingdom). All equipment and apparatus were available at the University of Dar es Salaam. A scanning electron microscope (SEM, Hitachi S-4800) was accessed from African Minerals and Geosciences Centre, Dar es Salaam.

Methods

Sample Preparation

White waste cotton fabric pieces were collected from 21st Textile Mills in Morogoro. The collected clothes were cleaned in an aqueous solution containing 10 g/L of sodium lauryl sulfate detergent and 3.0 g/L of hydrogen peroxide at a temperature of 30 °C for 3 min. The washed cotton fabrics were rinsed with distilled water for 2 min and then oven-dried at 80 °C for 30 min (Peila et al. 2015). The cleaned fabrics were cut manually into small pieces (approximately 2 × 2 mm), followed by the mechanical breaking of the fabric pieces into their constituent fibres using the ES-2255 blender before dissolution (Wang et al. 2022).

Partial Dissolution of the Cotton Fibres

To obtain a highly porous membrane, partial dissolution of cotton fibres was done by adding activated cotton fibres (1.0 and 1.6 w/v) to the DMAc solution with constant stirring at 60 to 80 ˚C for 1 hour to allow penetration of the solvent into the fibres. The suspension was allowed to cool to 60 ˚C, and then 8.5% of anhydrous LiCl (oven-dried at 200 ˚C for 1 hour) was added (Dupont 2003). The cotton cellulose suspension was further stirred at 400 rpm for a period of between 16 and 20 hours at approximately 80 ˚C to achieve partial dissolution of the cotton fibres (Duchemin 2008; Rebière et al. 2016).

Fabrication of Fibrous Membrane

To produce a homogeneous suspension, a suspension of partially dissolved fibres was mixed with 50 mL of DMAc and stirred for 30 min. The resulting suspensions were filtered through Millipore membranes with a pore size ranging from 0.45 to 0.65 µm. The millipore membranes were supported with a metallic sieve with pore sizes of 110 µm (Huang 2018). The filtration time of the suspension was controlled for 5 min. After filtration, the wet filter cellulose cake was wet-pressed and dried for 1 hour at a temperature of 100 ºC in an oven (Hassan et al. 2020).

Thickness Measurement

The thickness of the membrane was measured by using the digital thickness gauge. The thickness was measured by holding the workpiece between the stylus and anvil, and the thickness was taken at five different positions, and the average value was calculated.

Measurement of Density and Porosity of the Membrane

The density of the microporous membrane was determined by measuring the membrane weight (air-dry weight, containing moisture) and dividing it by its volume. The volume was calculated from the thickness of the porous membrane and its area. The percentage porosity (P) was estimated from the density of the porous membrane (ρ_m) by taking 1.54 g/cm^3 as the density of cellulose (ρ_c) using Equation (1) (Hossen et al. 2020).

$$P = \left(1 - \frac{\rho_m}{\rho_c}\right) \times 100\% \qquad (1)$$

Fibre Length Analysis

A Biobase light microscope (model RMB-117M)) coupled with scope image 9.0 software for capturing an image (Image J

software) was used to measure the fibre length and diameter of the partially dissolved fibres (Le Van 2017). The OriginPro 8.5 software was used to analyse the fibre length and diameter distributions.

Characterization of Surface Morphology

The surface morphology of the fabricated microporous membranes was investigated by scanning electron microscopy (SEM, Hitachi S-4800). The samples were coated with graphite and gold-palladium using Agar HR sputter coaters to allow spatial scattering of electric charges on the surface of the specimen and clear image production. A secondary electron detector was used for capturing the images at 10 kV.

Analysis of Chemical Functional Groups

Fourier Transform Infrared Spectrometer (FT-IR) was applied to investigate the microporous membranes' surface chemistry. FTIR was set at the absorbance spectra range of 4000–400 cm $^{-1}$ (64 scans, absorption mode). A diamond attenuated total reflection (ATR) optical unit was used to analyse and compare cotton fabrics' chemical structure with the microporous cellulose membrane samples.

Membrane Performance

Microporous membranes prepared at different concentrations and times were tested for filtration efficiency against NaCl particles. The laboratory-prepared sodium chloride solution at a concentration of 500 ppm was passed through the membrane using the dead-end stirred cell at 25 °C. A differential pressure of 0.2 MPa was maintained using a vacuum pump, where the active filtration area was 12.56 cm^2. Absorbance was measured before and after passing the NaCl particles through the membranes using a Jenway 7205 UV–visible spectrometer. A standard curve of concentration versus absorbance at 540 nm was set for a series of NaCl solutions with known concentrations. The concentration of NaCl in the filtrate was calculated from a standard curve equation. Rejection efficiency (r) against the NaCl particles was calculated from initial (C_i) and final (C_f) concentrations using Equation (2) (Hassan et al. 2020).

$$r(\%) = \frac{C_i - C_f}{C_i} \times 100\% \qquad (2)$$

RESULTS AND DISCUSSION

Figures 1 and 2 show the fibre length and diameter distributions of cotton fibres at different dissolution times and temperatures. Figures 1(a) and 2(a) show the original state of the fibres before dissolution. An optical microscope was used to capture the image of cotton fibres in the solution of DMAc/LiCl. It was observed that all cellulose fibres had a microscale dimension, which is an ideal size for application in filter membranes. The diameters and lengths of cellulose fibres were determined using Image J software. The results indicated that the length and diameter decreased drastically by increasing the dissolution time. This agrees well with the fibre size of the starting materials, as shown in Figures 1(a) and 2(a). According to (Ghasemi et al. 2017), at higher dissolution times (above 20 hrs), the fibres dissolve completely due to the elimination of large parts of the amorphous domains and some parts of the crystalline domains, reducing the fibres to nanofibres or nanocrystals.

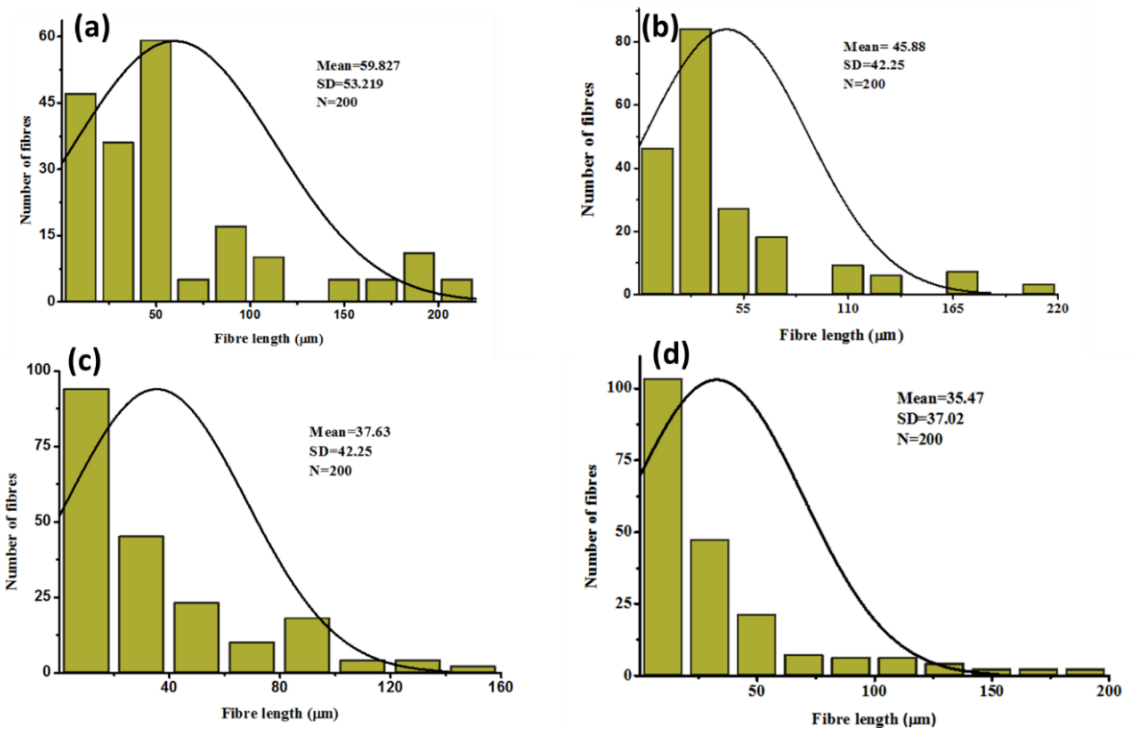

Figure 1: (a) Fibre length distribution of undissolved cotton fibre. Fibre length distribution of partially dissolved cotton fibres in DMAc/LiCl solution for (b) 16, (c) 18, and (d) 20 hrs at a temperature of 80 °C.

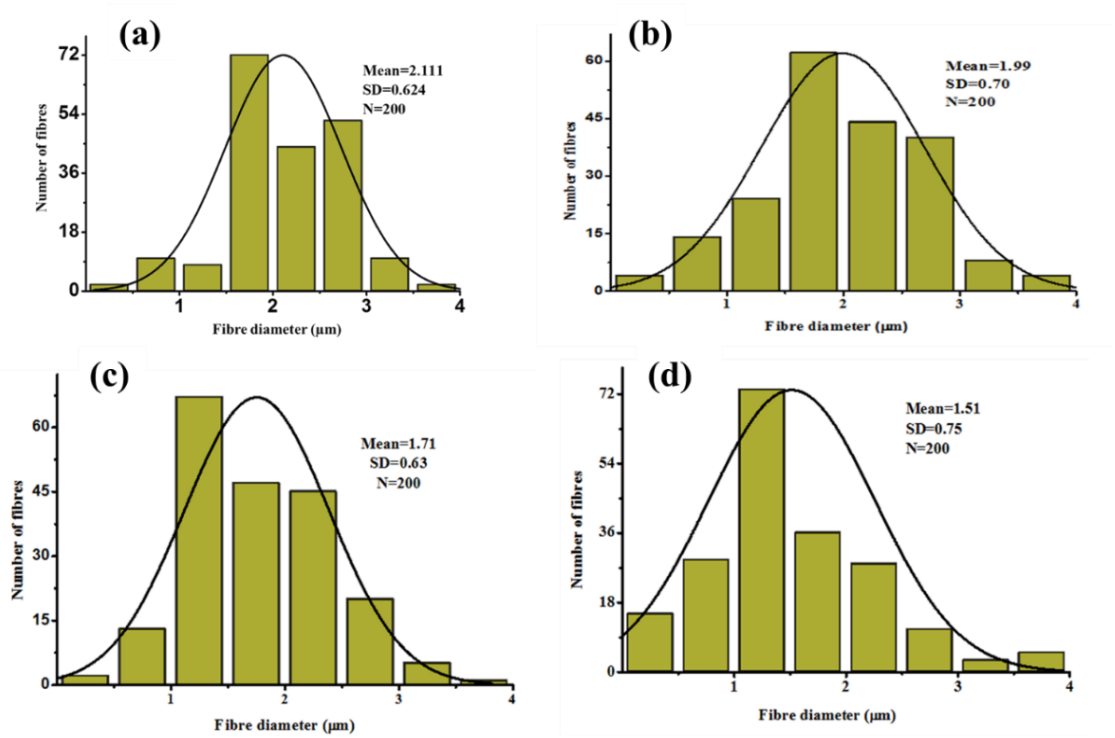

Figure 2: (a) Fibre diameter distribution of undissolved cotton fibres. Fibre diameter distributions of cotton fibres partially dissolved in DMAc/LiCl solution for (b) 16, (c)18 and (d) 20 hrs at a temperature of 80 °C.

FT-IR spectra of cotton cellulose fibres and porous membranes were utilized to further examine the influence of dissolution and the structure of cellulose membranes. Figure 3 shows two peaks at 3265 cm^{-1} and 3344 cm^{-1} attributed to intramolecular hydrogen bonds in the cellulose structure. Peaks at 1431, 1364, 1333, and 1314 cm^{-1} may be attributed to CH_2 bending, CH bending, OH bending, and CH_2 rocking vibration, as reported by (Phinichka and Kaenthong 2018). The disappearance of the characteristic band at 1431 cm^{-1} indicates a shift in cellulose crystalline structure after the dissolution. The band intensity at 895 cm^{-1}, which represents amorphous cellulose, increased similar to previous results (Wang et al. 2022). It can be seen that the absorbance of the hydroxyl functional group on the cellulose membrane at 3397.34 cm^{-1} is greater than that of pure cellulose, and the peak at 1639.58 cm^{-1} indicates HOH hydration probably due to the presence of lithium chloride in the cellulose membrane as also observed earlier (Laksono and Aji 2016). Furthermore, the absorbance peaks at 541.31 and 592.71 cm^{-1} indicate the presence of lithium (Laksono and Aji 2016).

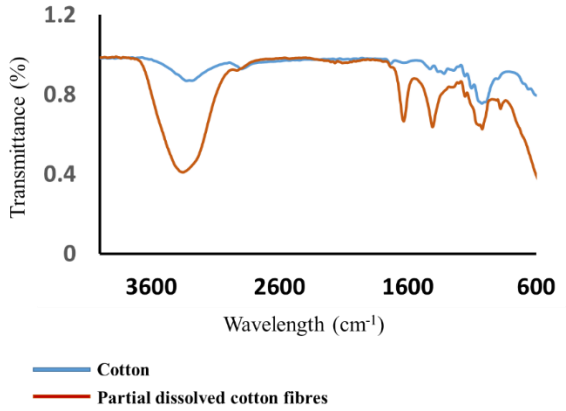

Figure 3: FTIR profiles of cellulose and porous cellulose membrane.

Figure 4 shows the optical microscope images of cellulose membranes. The membranes exhibit continuous random network fibres free of macroscopic agglomeration and defects, as shown in Figure 4(a1-c1). The membranes produced from the concentration of 1.0, 1.3, and 1.6 % at a dissolution time of 16 hrs [Figure 4(a1-3)], showed less intact fibres on their surfaces compared to the membranes containing fibres that were partially dissolved for 18 and 20 hrs, as shown in [Figure 4(b1-3)] and [Figure 4(c1-3)], respectively. This can be attributed to the presence of a smaller number of dissolved fibres that act as a binder or matrix to hold the undissolved fibres together. The thickness and compactness of the membrane increased with the concentration from 1.0 to 1.3 and 1.6%. The effect of the concentration was further investigated by determining the porosity (%) of the fabricated membranes.

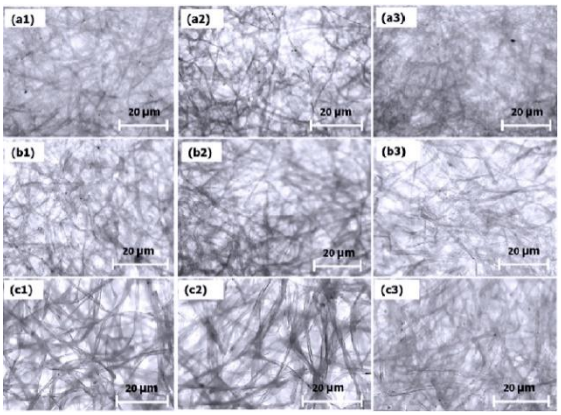

Figure 4: Optical microscopic images of porous cellulose membranes prepared from DMAc/LiCl solutions containing cotton fibres at concentrations of (a) 1.0, (b) 1.3 and (c) 1.6% partially dissolved for (a1-3) 16, (b1-3) 18 and (c1-3) 20 hrs at **at a temperature of 80 °C.**

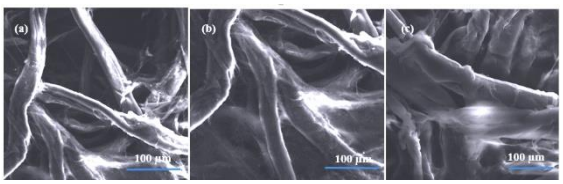

Figure 5: SEM micrographs of the microporous membranes obtained after a partial dissolution of (a) 1.0%, (b) 1.3%, and (c) 1.6% of cotton for 18 hrs at a temperature of 80 ˚C and concentration of

The network structure of the microporous membranes was examined by using SEM, as shown in Figure 5(a-c). The membranes

exhibited a random network of cellulose nanofibrils with notable differences in morphology and dimensions. As shown in Figure 5(a-c), membranes prepared from 1.0% concentration were less dense than those obtained from 1.3 and 1.6%. Moreover, the size of the fibres in the membrane is worth considering because the smaller the fibre diameter, the smaller the porosity of the membrane (Aizawa and Wakui 2020; Tarus et al. 2020) .

The density and porosity of the fibrous membranes were determined, as shown in Table 1. Fibrous cellulose membranes with low density transformed into membranes with higher density and less porosity as the dissolution time increased. The increase in the membrane density resulted from the filling of the pores of the membrane by smaller cellulose fibres. On the other hand, the porosity of the membrane decreased with the increase in fibre content due to fewer and smaller pores caused by entangled fibres within the membranes (Song et al. 2022). The decrease in porosity indicated that the increase in the cellulose content could control the porosity of the membrane. The pore size in the membrane decreased when higher fibre concentrations were used.

Table 1: The influence of concentration and dissolution time on the porosity and density properties of the microporous cellulose membranes.

S/N	Time (hrs)	Concentration (w/v %)	Temperature (˚C)	Thickness (cm)	Volume (cm^3)	Density ($g/(cm^3)$)	Porosity (%)
1	16	1.3	80	0.02	0.04	0.57	63.27
2	18	1.3	80	0.02	0.04	0.58	62.60
3	20	1.3	80	0.02	0.04	0.61	60.21
4	16	1.3	70	0.02	0.05	0.55	64.56
5	18	1.3	70	0.02	0.05	0.55	64.24
6	20	1.3	70	0.02	0.04	0.56	63.60
7	16	1.3	60	0.03	0.05	0.46	69.94
8	18	1.3	60	0.03	0.05	0.50	67.40
9	20	1.3	60	0.02	0.05	0.53	65.46

Sodium chloride was used to mimic the size of pathogens in droplet form to validate the performance of the membrane as a potential filter for pathogens. The particles existed as droplets with diameters of 0.1-100 µm (Weis and Ewing 1999). Table 2 shows that the filtration efficiency was widely dependent on the membrane fabrication process. Membranes produced with a higher amount of cotton fibres performed better compared to those with a small number of fibres. However, the filtration performance of the membrane eventually declined with the reduction in the dissolution temperature. A decrease in filtration performance occurred due to the poor fibre-fibre bonding. Moreover, the filtration performance of the fibrous membranes depended on the fibre distribution. This is because the tight and thick packing of fibres provided better opportunities for fine particles to collide and adhere to the fibres, as supported by previous studies (Tcharkhtchi et al. 2021; Wang et al. 2021).

However, after five cycles of NaCl filtration, small fractures developed on the membrane surfaces due to the pressure applied during the filtration process. Pore size and pore diameter play important roles in NaCl filtration. The fibrous membrane of partially dissolved cotton fibres showed a good filtration performance of up to 70% compared to the filtration performance of hollow fibre nanofiltration membranes reported previously (Ismail and Lau 2009), which showed a filtration performance of 60%. This shows that the fibrous

membrane can be used in the filtration application of small-sized particles, including pathogens and aerosols (Yu et al. 2016).

Table 2: Filtration performance of fibrous membranes against sodium chloride solution

S/N	Time (hrs)	Concentration (w/v %)	Temperature (˚C)	Filtration (%)
1	18	1.0	80	12.06
2	18	1.3	80	59.85
3	18	1.6	80	70.32
4	18	1.0	70	7.39
5	18	1.3	70	35.05
6	18	1.6	70	46.21
7	18	1.0	60	10.81
8	18	1.3	60	31.83
9	18	1.6	60	40.18

CONCLUSION

Fibrous cotton membranes were prepared from partially dissolved cotton fibres using a ‘vacuum filtration’ method, followed by hot-pressing of the membranes. Scanning electron microscopy revealed well-dispersed randomized cotton fibres on the surface of the membranes and completely dissolved cotton fibres which acted as binders. The hot-pressing process of the membranes increased their compactness. Partial dissolution of the cotton fibres reduced the length of the fibres and the sodium chloride solution flux to the fabricated membranes. The formed membranes showed a decrease in porosity with an increase in the cellulose content, dissolution time, and temperature. The prepared membranes showed a promising ability to remove particles (NaCl) from water. Membrane fabrication via vacuum filtration followed by hot pressing introduced a cost-effective method that enabled reasonable rejection rates of sodium chloride particles. Further optimization of pore sizes and thickness of the fabricated membranes may bring them to a commercially viable level for filtration of nano to micro-particulate matters, including pathogens and aerosols. Therefore, this study provides a new way of utilizing cotton waste to develop biodegradable and environmentally friendly membranes for pathogen/aerosol filtration. The findings in this article have not been tested directly against pathogens (bacteria and viruses).

Acknowledgements
This work was supported by the University of Dar es Salaam through Competitive Research and Innovation Grants for 2020-2021.

Conflicts of Interest: The authors declare no conflict of interest.

REFERENCES

Adil, T., Rahman, R., Whitelaw, D., Jain, V., Al-Taan, O., Rashid, F., Munasinghe, A., and Jambulingam, P. (2021). SARS-CoV-2 and the Pandemic of COVID-19. *Postgraduate Medical Journal*, **97**(1144): 110-116. DOI:

10.1136/postgradmedj-2020-138386

Aizawa, T., and Wakui, Y. (2020). Correlation Between the Porosity and Permeability of A Polymer Filter Fabricated via CO_2-

Assisted Polymer Compression. *Membranes*, **10**(12): 391. DOI: 10.3390/membranes10120391.

Bolashikov, D., and Melikov, K. (2009). Methods for Air cleaning and Protection of Building Occupants from Airborne Pathogens. *Building and Environment*, **44**(7): 1378-1385. DOI: 10.1016/j.buildenv.2008.09.001.

Bonfim, P., Cruz, G., Guerra, G., and Aguiar, L. (2021). Development of Filter Media by Electrospinning for Air Filtration of Nanoparticles from PET Bottles. *Membranes*, **11**(4): 293. DOI: 10.3390/membranes11040293.

Borojeni, A., Gajewski, G., and Riahi, A. (2022). Application of Electrospun Nonwoven Fibers in Air Filters. *Fibers*, **10**(2): 15. DOI: 10.3390/fib10020015.

Cornelio, A., Zanoletti, A., Federici, S., Ciacci, L., Depero, E., and Bontempi, E. (2022). Environmental Impact of Surgical Masks Consumption in Italy Due to COVID-19 Pandemic. *Materials*, **15**(6): 2046. DOI: 10.3390/ma15062046.

Duchemin, C. (2008). Structure, Property and Processing Relationships of All-Cellulose Composites. PhD Thesis. University of Canterbury Christchurch New Zealand. DOI: 10.26021/1603.

Dupont, A-L. (2003). Cellulose in Lithium Chloride/N, N-dimethylacetamide, Optimisation of a Dissolution Method Using Paper Substrates and Stability of the Solutions. *Polymer*, **44**(15): 4117-4126. DOI: 10.1016/S0032-3861(03)00398-7.

Fan, X., Wang, Y., Zheng, M., Dunne, F., Liu, T., Fu, X., Kong, L., Pan, S., and Zhong, H. (2018). Morphology Engineering of Protein Fabrics for Advanced and Sustainable Filtration. *Journal of Materials Chemistry A*, **6**(43): 21585-21595. DOI: 10.1039/C8TA08717B.

Ghasemi, M., Tsianou, M., and Alexandridis, P. (2017). Assessment of Solvents for Cellulose Dissolution. *Bioresource Technology*, **228:** 330-338. DOI:10.1016/j.biortech.2016.12.049.

Giovambattista, N., Rossky, J., and Debenedetti, G. (2009). Effect of Temperature on the Structure and Phase Behavior of Water Confined by Hydrophobic, Hydrophilic, and Heterogeneous Surfaces. *The Journal of Physical* Chemistry *B*, **113**(42): 13723-13734.DOI: 10.1021/jp9018266.

Gopakumar, A. (2017). Nanocellulose Based Functional Constructs for Clean Water and Microwave Suppression. Unpublished, Université de Bretagne Sud; Mahatma Gandhi University.

Hassan, L., Fadel, M., Abouzeid, E., Abou Elseoud, S., Hassan, A., Berglund, L., and Oksman, K. (2020). Water Purification Ultrafiltration Membranes Using Nanofibers from Unbleached and Bleached Rice Straw. *Scientific Reports*, **10**(1): 1-9. DOI:10.1038/s41598-020-67909-3.

Hossen, R., Talbot, W., Kennard, R., Bousfield, W., and Mason, D. (2020). A Comparative Study of Methods for Porosity Determination of Cellulose Based Porous Materials. *Cellulose*, **27**(12): 6849-6860. DOI: 10.1007/s10570-020-03257-9.

Huang, W. (2018). Cellulose nanopapers. in *Nanopapers*: Elsevier. pp. 121-173. DOI 10.1016/B978-0-323-48019-2.00005-0.

Ijaz, K., Zargar, B., Wright, E., Rubino, R., and Sattar, A. (2016). Generic Aspects of the Airborne Spread of Human Pathogens Indoors and Emerging Air Decontamination Technologies. *American Journal of Infection Control*, **44**(9): S109-S120. DOI: 10.1016/j.ajic.2016.06.008.

Ismail, A., and Lau, W. (2009). Influence of Feed Conditions on the Rejection of Salt and Dye in Aqueous Solution by Different Characteristics of Hollow Fiber Nanofiltration Membranes. *Desalination and Water Treatment*, **6**(1-3):281-288.DOI:10.5004/DWT.2009.479.

Kaur, R., and Pandey, P. (2021). Air Pollution, Climate Change, and Human Health in Indian Cities: A Brief Review. *Frontiers in Sustainable Cities*, **3:** 705131. DOI: 10.3389/frsc.2021.705131.

Laksono, W., and Aji, D. (2016). Conductivity of Cellulose Acetate Membranes from Pandan Duri Leaves (Pandanus Tectorius) for Li-Ion Battery. in *MATEC Web of Conferences*: EDP Sciences. pp. 04001. DOI: 10.1051/matecconf/20166404001.

Le Van, H. (2017). Properties of Nano-Fibrillated Cellulose and Its Length-Width Ratio Determined by a New Method. *Cellulose Chemistry and Technology*, **51**(7-8): 649-653.

Li, G., Fang, C., Wang, S., and Sun, S. (2016). The Effect of Economic Growth, Urbanization, and Industrialization on Fine Particulate Matter (PM2. 5) Concentrations in China. *Environmental Science & Technology*, **50**(21): 11452-11459. DOI: 10.1021/acs.est.6b02562

Liu, B., Zhang, S., Wang, X., Yu, J., and Ding, B. (2015). Efficient and Reusable Polyamide-56 Nanofiber/Nets Membrane with Bimodal Structures for Air Filtration. *Journal of Colloid and Interface Science*, **457:** 203-211. DOI: 10.1016/j.jcis.2015.07.019.

Mautner, A., Lee, Y., Tammelin, T., Mathew, P., Nedoma, J., Li, K., and Bismarck, A. (2015). Cellulose Nanopapers as Tight Aqueous Ultra-Filtration Membranes. *Reactive and Functional Polymers*, **86:** 209-214. DOI: 10.1016/j.reactfunctpolym.2014.09.014.

Noor, R., and Maniha, S. M. (2020). A Brief Outline of Respiratory Viral Disease Outbreaks: 1889–Till Date on the Public Health Perspectives. *VirusDisease*, **31**(4): 441-449. DOI: 10.1007/s13337-020-00628-5.

Pandit, P., Maity, S., Singha, K., Uzun, M., Shekh, M., and Ahmed, S. (2021). Potential Biodegradable Face Mask to Counter Environmental Impact of Covid-19. *Cleaner Engineering and Technology*, **4:** 100218. DOI: 10.1016/j.clet.2021.100218.

Peila, R., Grande, A., Giansetti, M., Rehman, S., Sicardi, S., and Rovero, G. (2015). Washing off Intensification of Cotton and Wool Fabrics by Ultrasounds. *Ultrasonics Sonochemistry*, **23:** 324-332. DOI: 10.1016/j.ultsonch.2014.09.004.

Phinichka, N., and Kaenthong, S. (2018). Regenerated Cellulose from High Alpha Cellulose Pulp of Steam-Exploded Sugarcane Bagasse. *Journal of Materials Research and Technology*, **7**(1): 55-65. DOI: 10.1016/j.jmrt.2017.04.003.

Piscitelli, P., Miani, A., Setti, L., De Gennaro, G., Rodo, X., Artinano, B., Vara, E., Rancan, L., Arias, J., and Passarini, F. (2022). The Role of Outdoor and Indoor Air Quality in the Spread of SARS-Cov-2: Overview and Recommendations by the Research Group on COVID-19 and Particulate Matter (RESCOP Commission). *Environmental Research*, **211:** 113038. DOI: 10.1016/j.envres.2022.113038.

Power, L., Tennant, K., Jones, T., Tang, Y., Du, J., Worsley, T., and Love, J. (2018). Monitoring Impacts of Urbanisation and Industrialisation on Air Quality in the Anthropocene Using Urban Pond Sediments. *Frontiers in Earth Science*, **6:** 131. DOI: 10.3389/feart.2018.00131.

Rebière, J., Heuls, M., Castignolles, P., Gaborieau, M., Rouilly, A., Violleau, F., and Durrieu, V. (2016). Structural Modifications of Cellulose Samples After Dissolution into Various Solvent Systems. *Analytical and bioanalytical chemistry*, **408**(29): 8403-8414.DOI:10.1007/s00216-016-9958-1.

Saadat, S., Rawtani, D., and Hussain, M. (2020). Environmental Perspective of COVID-19. *Science of the Total Environment*, **728:** 138870. DOI: 10.1016/j.scitotenv.2020.138870.

Sanyal, A. and Sinha-Ray, S. (2021) Ultrafine PVDF Nanofibers for Filtration of Air-Borne Particulate Matters: A Comprehensive Review. *Polymers*, **13**(11): 1864. DOI: 10.3390/polym13111864.

Selvaranjan, K., Navaratnam, S., Rajeev, P., and Ravintherakumaran, N. (2021). Environmental Challenges Induced by Extensive Use of Face Masks During COVID-19: A Review and Potential Solutions. *Environmental Challenges*, **3:** 100039. DOI: 10.1016/j.envc.2021.100039.

Song, Y., Seo, Y., Kim, H., Cho, S., and Baek, Y. (2022). Pore-Size Control of Chitin Nanofibrous Composite Membrane Using Metal-Organic Frameworks. *Carbohydrate Polymers*, **275**(20): 118754. DOI: 10.1016/j.carbpol.2021.118754.

Tarus, K., Fadel, N., Al-Oufy, A., and El-Messiry, M. (2020). Investigation of Mechanical Properties of Electrospun Poly (Vinyl Chloride) Polymer Nanoengineered Composite. *Journal of Engineered Fibers and Fabrics*, **15**: 1-10. DOI: 10.1177/1558925020982569.

.Tcharkhtchi, A., Abbasnezhad, N., Seydani, Z., Zirak, N., Farzaneh, S., and Shirinbayan, M. (2021). An Overview of Filtration Efficiency through the Masks: Mechanisms of the Aerosols Penetration.

Bioactive Materials, **6**(1): 106-122. DOI: 10.1016/j.bioactmat.2020.08.002.

Tesfaldet, T., and Ndeh, T. (2022). Assessing Face Masks in the Environment by Means of the DPSIR Framework. *Science of the Total Environment*, **814**: 152859. DOI: 10.1016/j.scitotenv.2021.152859.

Wang, J., Liu, S., Yan, X., Jiang, Z., Zhou, Z., Liu, J., Han, G., Ben, H., and Jiang, W. (2021). Biodegradable and Reusable Cellulose-Based Nanofiber Membrane Preparation for Mask Filter by Electrospinning. *Membranes*, **12**(1): 23. DOI:10.3390/membranes12010023.

Wang, L., Huang, S., and Wang, Y. (2022). Recycling of Waste Cotton Textile Containing Elastane Fibers through Dissolution and Regeneration. *Membranes*, **12**(4): 355. DOI: 10.3390/membranes12040355.

Wang, N., Cai, M., Yang, X., and Yang, Y. (2018). Electret Nanofibrous Membrane with Enhanced Filtration Performance and Wearing Comfortability for Face Mask. *Journal of Colloid and Interface Science*, **530:** 695-703. DOI: 10.1016/j.jcis.2018.07.021.

Weis, D., and Ewing, E. (1999). Water Content and Morphology of Sodium Chloride Aerosol Particles. *Journal of Geophysical Research: Atmospheres*, **104**(D17): 21275-21285. DOI:10.1029/1999JD900286.

Xiao, H., Song, Y., and Chen, G. (2014). Correlation Between Charge Decay and Solvent Effect for Melt-Blown Polypropylene Electret Filter Fabrics. *Journal of Electrostatics*, **72**(4): 311-314. DOI: 10.1016/j.elstat.2014.05.006.

Yu, W., Brown, M., and Graham, N. (2016). Prevention of PVDF Ultrafiltration Membrane Fouling by Coating MnO_2 Nanoparticles with Ozonation. *Scientific Reports*, **6**(1): 1-12. DOI: 10.1038/srep30144.

Zhou, Y., Liu, Y., Zhang, M., Feng, Z., Yu, G., and Wang, K. (2022). Electrospun Nanofiber Membranes for Air Filtration: A Review. *Nanomaterials*, **12**(7): 1077. DOI: 10.3390/nano12071077.